Innovative superparamagnetic iron-oxide nanoparticles coated with silica and conjugated with linoleic acid: Effect on tumor cell growth and viability

Innovative superparamagnetic iron-oxide nanoparticles coated with silica and conjugated with linoleic acid: effect on tumor cell growth and viability

Giuliana Muzio[a], Marta Miola*[b,d], Sara Ferraris*[b], Marina Maggiora[a], Elisa Bertone[b], Maria Paola Puccinelli[c], Marina Ricci[a], Ester Borroni[d], Rosa Angela Canuto*[a], Enrica Vernè*[b], Antonia Follenzi*[d]

[a] Department of Clinical and Biological Sciences, University of Turin, Corso Raffaello 30, 10125, Turin, Italy

[b] Department of Applied Science and Technology, Politecnico di Torino, Corso Duca degli Abruzzi 24, 10129 Turin, Italy

[c] Department of Laboratory Medicine, Azienda Ospedaliera Universitaria, Città della Salute e della Scienza, Corso Bramante 88/90 10126 Turin, Italy

[d] Department of Health Sciences, University "Amedeo Avogadro" of East Piedmont, Novara, Italy

**co-shared authorship*

e-mail of authors:

Muzio G, giuliana.muzio@unito.it; Miola M, marta.miola@polito.it; Maggiora M, marina.maggiora@unito.it; Ferraris S, sara.ferraris@polito.it; Bertone E, elisa.bertone@polito.it; Puccinelli MP, mpuccinelli@cittadellasalute.to.it; Ricci M, marina.ricci@unito.it; Canuto RA, rosangela.canuto@unito.it; Vernè E, enrica.verne@polito.it; Follenzi A, antonia.follenzi@med.uniupo.it

Corresponding authors:

Prof. Enrica Vernè

Department of Applied Science and Technology,

Politecnico di Torino,

Corso Duca degli Abruzzi 24, 10129 Turin, Italy

Phone n. +39 011 5644717 e-mail: enrica.verne@polito.it

Prof. Antonia Follenzi

Department of Health Sciences,

University "Amedeo Avogadro" of East Piedmont,

Via Solaroli 17, 28100 Novara, Italy

Phone n. +39 0321 660674 e-mail: antonia.follenzi@med.uniupo.it

Abstract

One of the goals for the development of more effective cancer therapies with reduced toxic side effects is the optimization of innovative treatments to selectively kill tumor cells. The use of nanovectors loaded with targeted therapeutic payloads is one of the most investigated strategies. In this paper superparamagnetic iron oxide nanoparticles (SPIONs) coated by a silica shell or uncoated, were functionalized with single-layer and bi-layer conjugated linoleic acid (CLA). Silica was used to protect the magnetic core from oxidation, improve the stability of SPIONs and tailor their surface reactivity. CLA was used as novel grafting biomolecule for its anti-tumor activity and to improve particle dispersibility. Mouse breast cancer 4T1 cells were treated with these different SPIONs.

SPIONs functionalized with the highest quantity of CLA and coated with silica shell were the most dispersed. Cell viability was reduced by SPIONs functionalized with CLA in comparison with cells which were untreated or treated with SPIONs without CLA. As regards the types of SPIONs functionalized with CLA, the lowest viability was observed in cells treated with uncoated SPIONs with the highest quantity of CLA.

In conclusion, the silica shell free SPIONs functionalized with the highest amount of CLA can be suggested as therapeutic carriers because they have the best dispersion and ability to decrease 4T1 cell viability.

1. Introduction

Some progress has been made in the field of anticancer therapies, although the research on new strategies to find even more effective therapies and to reduce their toxic side effects is still needed. The development of innovative treatments to kill tumor or metastatic cells is a challenging goal and for this reason, several possible approaches are under investigation. Today nanomedicine-based therapies are used in cancer research because they can bypass cancer cell multi-drug resistance, poor solubility of hydrophobic anti-cancer drugs, and the use of dangerous radiations [1]. Cancer nanomedicine pays particular attention to superparamagnetic iron oxide nanoparticles (SPIONs), that can reach the tumor sites carrying chemotherapeutic drugs, nucleic acids, monoclonal antibodies, viral vectors engineered with therapeutic suicide genes or shRNAs [1,2,3]. SPIONs are also used for diagnostic assays, generation of local hyperthermia for tumor therapy or tissue repair by delivering stem cells [4,5]. In fact, SPIONs can be combined with contrast fluorescent agents to improve cancer cell imaging [1]. In hyperthermia therapy, SPIONs are localized near the cancer site by magnetic driving and can induce localized heating by an external alternating magnetic field. For example in "*in vitro*" experiments, 14 nm magnetic nanoclusters killed about 74% of MCF-7 cancer cells, by applying temperature of 45°C for 1 hour [6]. Similarly, a temperature of 43°C for about 17 minutes reduced the viability of HeLa cells exposed to an alternating magnetic field in the presence of silica coated iron oxide nanoparticles (NPs) [7]. SPIONs can be internalized in human mesenchymal stem cells without affecting viability and structure. Following this, the SPION-loaded stem cells can be attracted to specific sites by applying an external magnetic field [8].

When preparing SPIONs for the delivery of chemotherapeutic agents it is important to control their size, shape and surface properties, in order to assure their stability in solution and maintain superparamagnetic properties also in the presence of a variety of molecules. SPIONs which are smaller than 100 nm can easily circulate in the blood without being captured by reticulo-endothelial cells and can therefore selectively accumulate in the tumor microenvironment [3]. On the contrary

unmodified SPIONs tend to aggregate into large clusters and several studies suggest surface modification to avoid NP aggregation. A widely explored solution is surface coverage by polymers that has the unavoidable disadvantage of causing an increase in particle size and a potential loss in magnetic response [1]. Alternatively, small intermediary molecules can be used, acting as stabilizing agents and for the subsequent coupling of functional molecules.. Fatty acids, in particular oleic acid (OA), have been used as capping agent to obtain monodisperse SPIONs suspensions [9].

This study aimed to prepare functionalized SPIONs able to affect tumor cell viability. SPIONs, either coated with silica shell or uncoated, were prepared and functionalized with conjugated linoleic acid (CLA) in single- and bi-layer configuration. Silica was used for its ability to protect the magnetic core from oxidation, to improve the magnetite stability and to tailor the surface reactivity by improving biomolecule grafting [10]. CLA was chosen to improve SPION dispersion and to add an anticancer potential [11-13]. Fatty acids are crucial structural and functional cell components, and contribute to the functional/physical/chemical features of membranes [11-13]. Concerning cancer, it is well known that carcinogenesis is characterized by changes in fatty acid composition of membrane phospholipids.

2. Materials and Methods

2.1 Synthesis of superparamagnetic iron-oxide nanoparticles (Fe_3O_4)

Among the different methods for the SPIONs production, the co-precipitation process was selected since it is simple, rapid and allows a high yield. An aqueous solution of Fe^{2+} and Fe^{3+} salts in a 1:2 molar ratio was prepared by mixing $FeCl_2*4H_2O$ and $FeCl_3*6H_2O$ in bi-distilled water; subsequently the mixture was mechanically mixed at 300 rpm and Fe_3O_4 precipitation occurred by adding NH_4OH drop by drop, until the pH of the mixture reached about 10. The suspension was put in ultrasound for 20 minutes; subsequently an aliquot was washed twice with bi-distilled water to remove the unreacted reagents (Fe_3O_4), while the other aliquot was not washed (Fe_3O_4-NW).

2.2 One-step synthesis of conjugated linoleic acid-capped Fe_3O_4

In this procedure conjugated linoleic acid (CLA) was added in a single-step to the NP suspensions. A first synthesis of CLA-capped Fe_3O_4 NPs was carried out by adding drop by drop 3.0 µl of CLA/ml of NP suspension, to both washed (Fe_3O_4+CLA1) or not washed (Fe_3O_4-NW+CLA1), NP under mechanical mixing. A second synthesis (Fe_3O_4+CLA2) was performed using a higher amount of CLA (4.5 µl CLA/ml of NPs suspension). All suspensions were heated at 80 °C with stirring at 150 rpm for half hour. At the end of the functionalization process NP suspensions were washed twice with ethanol and re-suspended in bi-distilled water.

2.3 Two-step synthesis of conjugated linoleic acid-capped Fe_3O_4

In this procedure CLA was added in two steps to the NP suspensions. The two-step CLA-capped Fe_3O_4 NPs were synthesized by adding, in a second step, a further aliquot of CLA (3.0 µl CLA/ml of NP suspension) in the suspension of the one-step CLA-coated Fe_3O_4 NPs, both washed (Fe_3O_4+CLA1-TS) and not washed (Fe_3O_4-NW+CLA1-TS). The suspension was placed in orbital shaker at 80°C at 150 rpm for half hour. Subsequently, NPs were washed twice with ethanol and re-suspended in bi-distilled water, adjusting the pH at 12 by adding NH_4OH drop by drop [14].

2.4 Synthesis of silica-coated magnetite nanoparticles (Fe_3O_4-SiO_2)

In order to promote the single nanoparticles coating in a uniform way and obtain a stable suspension, Fe_3O_4 NPs were stabilized with 0.05 M citric acid. The pH was adjusted to 5.2 by dropwise NH_4OH and the suspension was placed 90 minutes at room temperature in orbital shaker (KS 4000i control, IKA®) at 150 rpm allowing the deprotonation of two carboxylic groups of citric acid and the bond to the OH groups exposed by Fe_3O_4 NPs [15]. Subsequently, citric acid-functionalized NPs were washed with bi-distilled water using an ultrafiltration device (Solvent

Resistant Stirred Cells - Merck Millipore) and re-suspended in bi-distilled water, adjusting the pH at about 10.1 to induce the deprotonation of the third carboxylic group, which allow an optimal NP dispersion. Then, magnetite NPs functionalized with citric acid were coated with a silica shell (Fe_3O_4-SiO_2) by sol-gel method, by adding TEOS (tetraethoxysilane) as silica precursor, ethanol as catalyst and water as solvent, to Fe_3O_4 NPs suspended in a water and ethanol solution (water: ethanol 1:4) [16]. The pH of suspension was adjusted at 10 (NH_4OH); the suspension was placed in orbital shaker at room temperature for 3 hours at 150 rpm. Subsequently, the Fe_3O_4-SiO_2 NPs were washed with bi-distilled water using an ultrafiltration device (Solvent Resistant Stirred Cells - Merck Millipore) and re-dispersed in water.

2.5 One-step synthesis of conjugated linoleic acid-capped Fe_3O_4-SiO_2

On the base of the results obtained for CLA coated Fe_3O_4, Fe_3O_4-SiO_2 were functionalized with the higher CLA amount (4.5 µl CLA/ ml of NPs) with one-step procedure (Fe_3O_4-SiO_2+CLA2). The suspension was heated at 80 °C and stirred at 150 rpm for half hour. At the end of the functionalization process CLA capped Fe_3O_4-SiO_2 NPs were washed twice with ethanol and re-suspended in bi-distilled water.

Table 1 resumes the name and samples composition. All chemicals were purchased from Sigma-Aldrich Co. (St Louis, MO, US).

Table 1: name and composition of the samples

Acronym	**NPs**	**Washing**	**CLA**	**CLA [µl] per 1 ml of NPs suspension**
Fe_3O_4+CLA1	Fe_3O_4	Yes	one-step	3.0
Fe_3O_4-NW+CLA1	Fe_3O_4	No	one-step	3.0
Fe_3O_4+CLA1-TS	Fe_3O_4	Yes	two-step	3.0
Fe_3O_4-NW+CLA1-TS	Fe_3O_4	No	two-step	3.0

Fe_3O_4+CLA2	Fe_3O_4	Yes	one-step	4.5
Fe_3O_4-SiO_2+CLA2	Fe_3O_4-SiO_2	Yes	one-step	4.5

2.6 Nanoparticles characterization

All synthesized NPs were subjected to morphological characterization by scanning transmission electron microscopy (STEM, MERLIN Zeiss – Germany). For STEM observation, a drop of diluted NP suspension was deposited on a copper TEM grid with carbon film (SPI Supplies® Brand Lacey Carbon Coated 200 Mesh Copper Grids – JEOL S.p.A.). Fourier transformation infrared spectroscopy (FT-IR) was used to evidence the effective grafting of CLA and to confirm the presence of silica shell. FT-IR spectra were acquired in a Hyperion 2000 FT/IR (Tensor 27, Bruker Optics S.p.A, Ettlingen, Germany) from 4000 to 400 cm^{-1} and with 2 cm^{-1} resolution. OPUS software (v. 6.5, Bruker S.p.A) was used for instrumental control and spectral acquisition. Suspension stability and dispersion were evaluated in a semi-quantitative way by measuring the time required for particle precipitation.

2.7 Cell Cultures: treatment of 4T1 with Fe_3O_4 NPs capped or not with CLA, or with CLA alone, and of MS1 cells with Fe_3O_4 NPs capped or not with CLA.

Mouse breast cancer 4T1 cells were seeded (12,500 cells/cm^2) in DMEM/F-12 medium supplemented with 2 mM glutamine, 1% (v/v) antibiotic/antimycotic solution, 10% (v/v) fetal bovine serum (FBS) and maintained at 37°C in a humidified atmosphere of 5% CO_2 in air. Twenty-four hours after seeding, culture medium was removed and replaced by the same medium not supplemented or supplemented with Fe_3O_4, Fe_3O_4-SiO_2, Fe_3O_4+CLA1, Fe_3O_4-NW+CLA1, Fe_3O_4+CLA1-TS, Fe_3O_4-NW+CLA1-TS, Fe_3O_4+CLA2 and Fe_3O_4-SiO_2+CLA2 at the concentrations 8 µg or 16 µg of NPs/100,000 cells. Twenty-four hours after seeding, the 4T1 cells

were also treated with CLA alone at 10 and 25 µM concentrations. The experimental times were 24, 48 and 72 hours.

Mouse pancreatic islet endothelial MS1 cells were seeded (12,500 cells/cm^2) in DMEM medium supplemented with 1% glutamine, 1% (v/v) antibiotic solution, 10% (v/v) fetal bovine serum (FBS) and maintained at 37°C in a humidified atmosphere of 5% CO_2 in air. Twenty-four hours after seeding, culture medium was removed and replaced by the same medium not supplemented or supplemented with Fe_3O_4, Fe_3O_4+CLA2, Fe_3O_4-SiO_2, and Fe_3O_4-SiO_2+CLA2 at the concentrations 8 µg or 16 µg of NPs/100,000 cells. The experimental times were 24, 48 and 72 hours.

2.7.1 Cell viability

Cell viability was evaluated by means of the MTT assay after 24, 48 and 72 hours of treatment, *4T1 or MS1* cells grown in multiwells were added with 30 µl of 4.5-dimethylthiazol-2-yl-,5 diphenyltetrazolium bromide (MTT, 5 mg/ml) in PBS solution, and incubated for 3 h at 37°C in a humidified atmosphere of 5% CO_2 in air. After the supernatants were removed and 150 µl of DMSO was added to each well. After 20 minutes of incubation, the absorbance was measured at 590 nm using a microplate reader (Dynatech MR580 microElisa, USA).

2.7.2 Iron staining

After 24 and 72 hours of treatment in chamber slides, the iron stain KIT HT20 (Sigma-Aldrich Co., St Louis, MO, USA) was used to evidence the SPIONs functionalized or not with CLA internalized by 4T1 and MS1 cells.

2.7.3 CLA percentage content in incubated cells

As indication of CLA-capped NP internalization, the CLA percentage content was determined in lipids extracted from $6x10^6$ cells previously incubated with Fe_3O_4, Fe_3O_4+CLA1, Fe_3O_4+CLA2 or

Fe_3O_4-SiO_2+CLA2 NPs for 72 hours. After treatment, the cells were washed with PBS+EDTA (0.53 mM), detached with trypsin/EDTA (0.25%/0.3%), and centrifuged at 600 g for 10 min at 4 °C.

Lipids, isolated by Folch et al. method [17], were suspended in 0.5 ml of methanol containing internal standard 1,2-dihenarachidoyl-sn-glycero-phosphocholine. The method of Klem et al. [18] for analysis of red blood cell fatty acid composition was adapted for the determination of CLA in 4T1 cell lipids. The extracts were evaporated under nitrogen flow, dissolved with chilled methanol containing 2,6 di-ter-butyl-4-methyl-phenol (BHT) as antioxidant, treated for 15 min in an ultrasound bath and then centrifuged. The supernatants were treated with a methanol solution of sodium methoxide to synthetize CLA methyl esters, and after 5 min a hydrochloric acid solution was added. CLA methyl esters were extracted twice with hexane, evaporated under nitrogen flow at 35° C, and re-dissolved in hexane containing BHT for injection in gas chromatograph–mass spectrometer. CLA were identified and quantified with a mass spectrometer operating in electron impact ionization (EI) mode. The selection of ions for selective ion monitoring (SIM) was based on comparison with standards and those reported in the literature [19, 20].

2.8 Statistical Analysis

All data are expressed as means ± SD. Differences between group means were assessed by analysis of variance followed by a post hoc Newman–Keuls test.

3. Results

3.1. Nanoparticles synthesis and characterization

The superparamagnetic properties and the XRD pattern of Fe_3O_4 NPs obtained with analogue procedure have been previously assessed [21]. Figure 1 shows STEM analyses of Fe_3O_4+CLA1, Fe_3O_4-NW+CLA1, Fe_3O_4+CLA1-TS, Fe_3O_4-NW+CLA1-TS, Fe_3O_4+CLA2 and Fe_3O_4-SiO_2+CLA2

NPs. All NPs present a spherical shape with a dimensional range of about 5-15 nm, with the exception of silica coated NPs, seeming slightly bigger (up to 20 nm). A silica shell (of about 1-2 nm) is well visible in the micrograph (last panel of figure 1) and is evidenced by arrows.

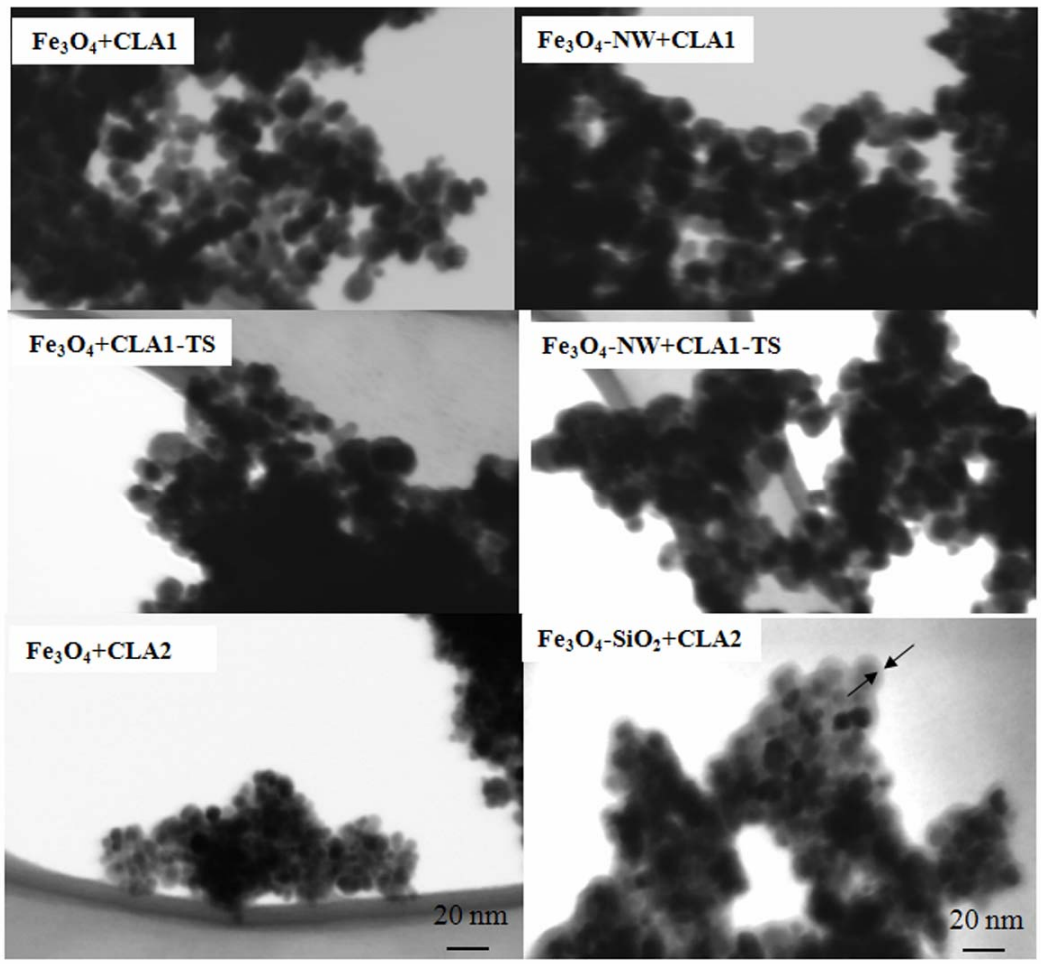

Figure 1. STEM images of SPIONs. Fe_3O_4+CLA1, washed CLA-capped Fe_3O_4 NPs; Fe_3O_4-NW+CLA1, not washed CLA-capped Fe_3O_4 NPs; Fe_3O_4+CLA1-TS, washed two step CLA-capped Fe_3O_4 NPs; Fe_3O_4-NW+CLA1-TS NPs, not washed two step CLA-capped Fe_3O_4 NPs; Fe_3O_4+CLA2; Fe_3O_4-SiO_2+CLA2, silica shell-coated, washed CLA-capped Fe_3O_4 NPs.

CLA1, 3.0 µl of CLA/ml of NPs; CLA2, 4.5 µl of CLA/ml of NPs.

FT-IR spectra of pure CLA, Fe_3O_4+CLA1, Fe_3O_4-NW+CLA1, Fe_3O_4+CLA1-TS, Fe_3O_4-NW+CLA1-TS are reported in Figure 2. Figure 2a shows the spectrum of CLA, in which two peaks

at about 2852 e 2922 cm^{-1} are assigned respectively to the asymmetric and symmetric stretching of CH_2; the peak at about 1710 cm^{-1} can be attributed to the C=O stretch vibration, the peak at 1460 cm^{-1} to the $–COO^-$ asymmetric stretch vibration [14], the peak at 1408 to the "umbrella" bending mode of CH_3 group [14], the band between 1250 and 1285 cm^{-1} can be associated to the presence of the C–O stretch or more generally to the vibration of the COOH group in oleic acid [22,23], the peaks at 981 and 945 cm^{-1} are characteristic of the *cis,trans* conjugated dienes [24] and the peak at about 720 cm^{-1} can be assigned both to CH_2 bending or rocking vibration and CH=CH vibration [24,23]. No significant differences can be observed in the FT-IR spectrum of pure CLA treated at 80°C (not reported), as a confirmation that the functionalization procedure does not alter the molecule. Figure 2b shows the whole spectrum for all NPs, showing peaks at about 560 cm^{-1}, ascribable to Fe-O stretching vibrational mode of Fe_3O_4, peaks at about 2852 e 2922 cm^{-1} that can be assigned respectively to the asymmetric and symmetric stretching of CH_2 group of CLA, and a peak at about 1408 cm^{-1} which can be ascribed to the "umbrella" bending mode of CH_3 group [14]. Focusing the analysis between 1000 and 4000 cm^{-1} (Figure 2c), it is possible to notice also the presence of a broad band at about 1500 - 1640 cm^{-1} that can be attributed to the asymmetric and symmetric stretch vibration of COO^- group reported in literature for fatty acids adsorbed on Fe_3O_4 [14,22]. Moreover, in the Fe_3O_4+CLA1-TS and Fe_3O_4-NW+CLA1-TS curves, the band at about 1250-1285 cm^{-1} and the peak at about 1710 cm^{-1} appeared (the first one ascribed to the C-O stretch vibration, or to the vibration of the COOH group in oleic acid [22,23], the second one to the C=O stretch vibration [14]).

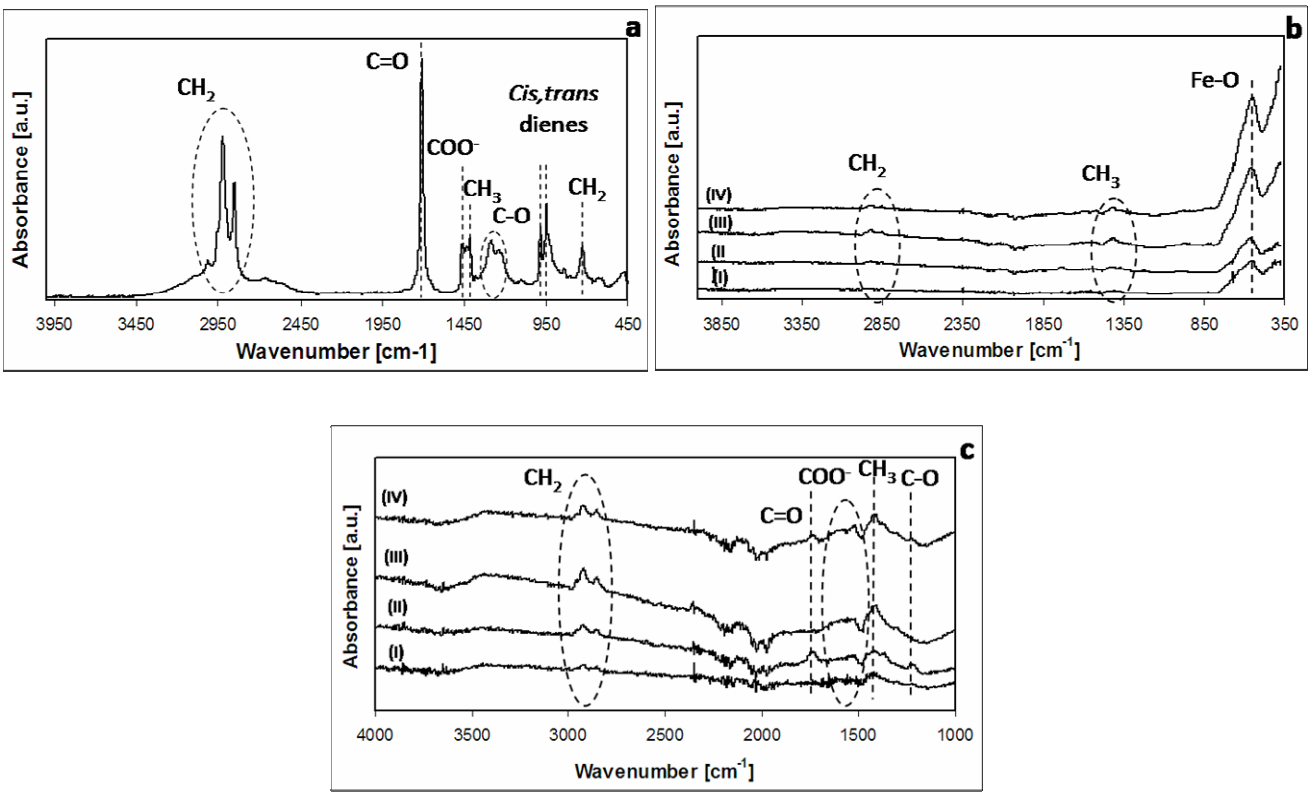

Figure 2. FT-IR spectra. (a) FT-IR spectra of pure CLA; (b) whole spectrum of Fe_3O_4-NW+CLA1 (curve I), Fe_3O_4-NW+CLA1-TS (curve II), Fe_3O_4+CLA1 (curve III), Fe_3O_4+CLA1-TS (curve IV) NPs; (c) selected windows between 1000 and 4000 cm^{-1}.

See legend in Figure 1 for NP acronyms.

The FT-IR spectra of Fe_3O_4+CLA2 and Fe_3O_4-SiO_2+CLA2 NPs are reported in Figure 3. The silica presence is evidenced by: a new peak at about 1060 cm^{-1} , attributed to the asymmetric stretching of the Si-O-Si group, two peaks at 960 and 780 cm^{-1} , attributed Si-OH stretching vibration and Si–O–Si symmetric stretching [25,26], and a band at about 3000-3300 cm^{-1} , ascribable to OH groups. The peaks at 2852 e 2922 cm^{-1} can be assigned respectively to the asymmetric and symmetric stretching of CH_2 group of CLA, the band at about 1500 - 1640 cm^{-1}, attributed to the asymmetric and symmetric stretch vibration of adsorbed COO^- group [14,22], and the peak at about 1408 cm^{-1}

ascribed to the “umbrella” bending mode of CH_3 group. Also in this samples the peak at about 1710 cm^{-1}, ascribable to the C=O vibration of CLA, appears.

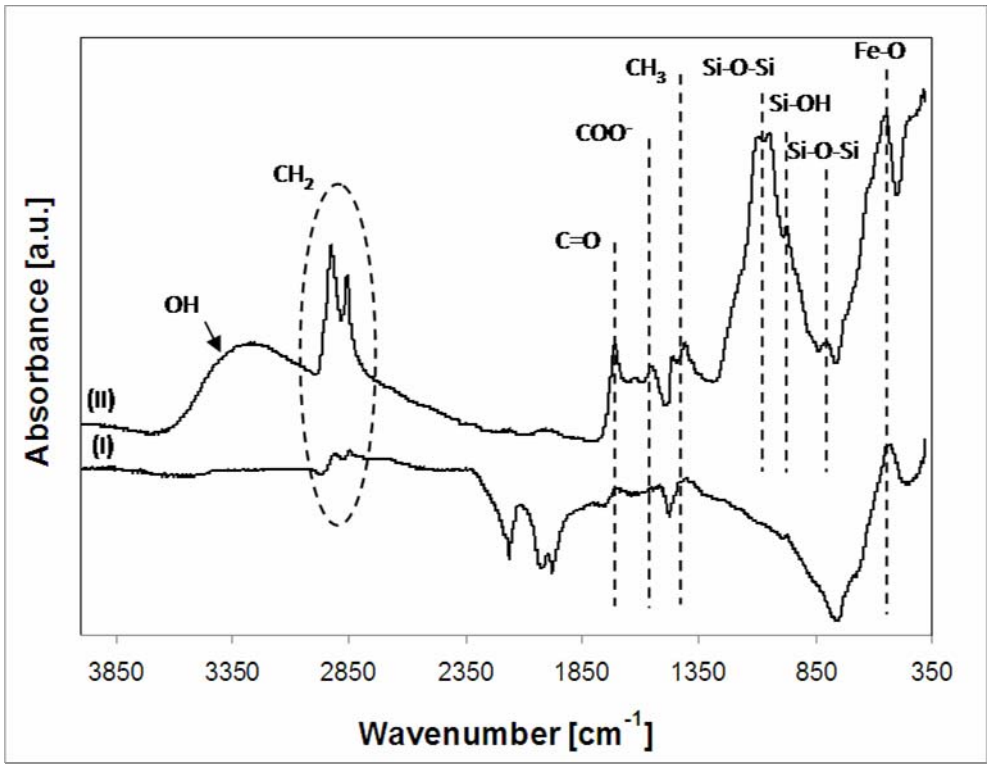

Figure 3. FT-IR spectra. FT-IR spectra of Fe_3O_4+CLA2 (curve I) and Fe_3O_4-SiO_2+CLA2 (curve II) NPs.

See legend in Figure 1 for NP acronyms.

Figure 4 reports the behavior of the various NP suspensions after different times of sedimentation. The precipitation of Fe_3O_4+CLA1 NPs starts after 5 minutes and is already complete after 30 minutes. The Fe_3O_4+CLA2 and Fe_3O_4-SiO_2+CLA2 solutions are both still stable after 2 hours, and only Fe_3O_4-SiO_2+CLA2 also after 24 hours.

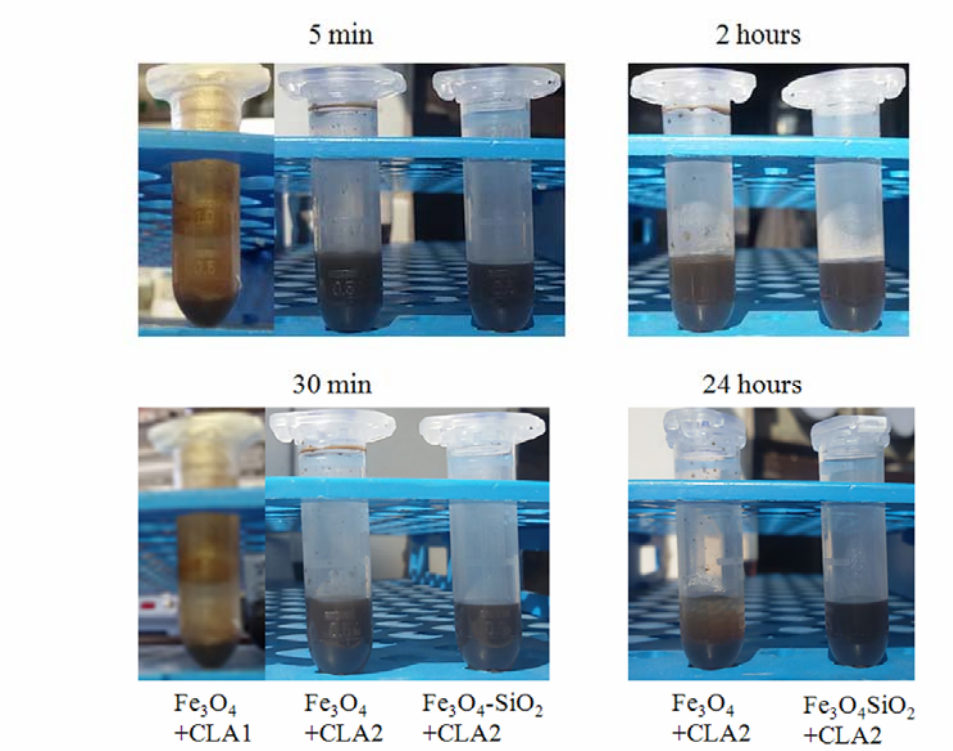

Figure 4. Precipitation of SPIONs. Time of precipitation of NPs with or without silica, capped or not with CLA. See table 1 for NPs acronyms.

3.2 The effect of SPIONs and CLA alone on mouse breast cancer 4T1 cells and on mouse pancreatic islet endothelial MS1 cells.

SPIONs, washed or not, and SPIONs functionalized with CLA (low and high amount, one- or two-steps) were tested to choose the preparation showing the highest inhibition of 4T1 cell proliferation. All functionalized particles decrease cell number in comparison with SPIONs not functionalized with CLA (Fe_3O_4), being the major inhibition obtained by SPIONs washed and capped with CLA with one-step procedure (data not shown). Therefore, in the following experiments, only Fe_3O_4, Fe_3O_4+CLA1 and Fe_3O_4+CLA2, with or without silica shell, were compared.

Figure 5 shows the percentages of viability in cells treated with various SPIONS in comparison with the control cells, set to 100%. The viability in cells treated with Fe_3O_4+CLA1, Fe_3O_4+CLA2 or Fe_3O_4-SiO_2+CLA2 is lower than in control cells and in cells treated with Fe_3O_4 and Fe_3O_4-SiO_2.

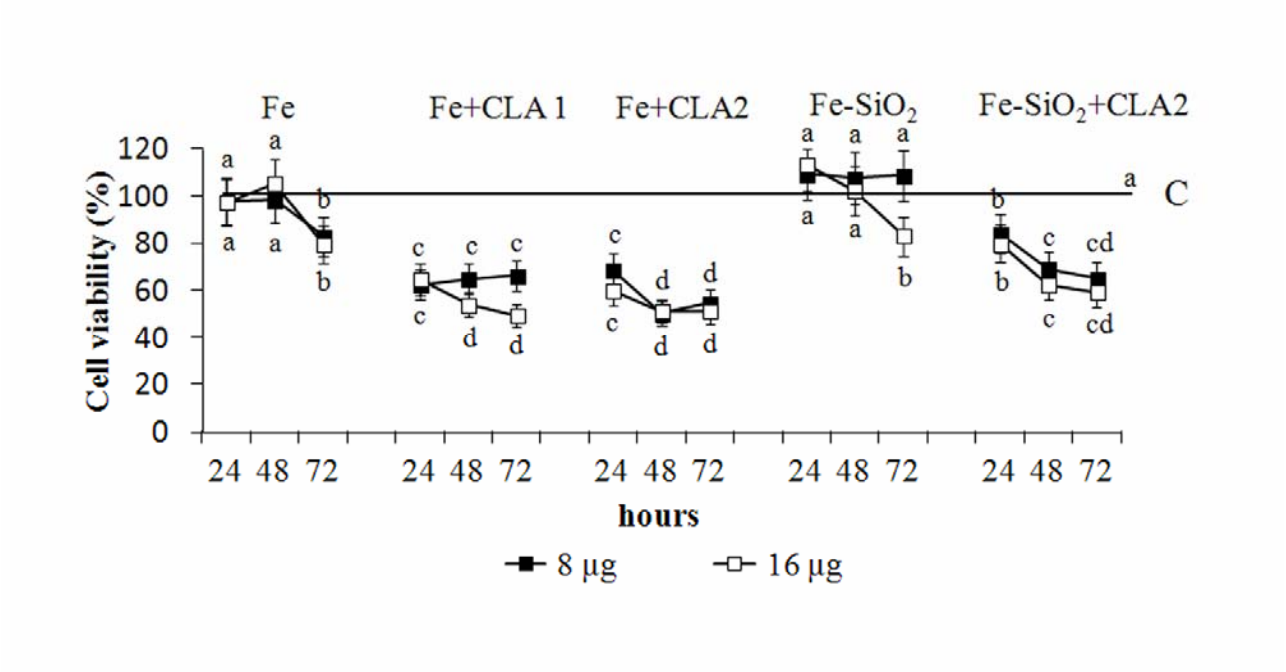

Figure 5 Viability of mouse breast cancer 4T1 cells exposed to Fe_3O_4 NPs coated or not with silica and capped or not with CLA. The values are means ± S.D. of 4 experiments and are expressed as % of control cells set equal to 100 %. The absorbance values of control are 0.591 ± 0.192 for 24 hours, 1.457 ± 0.151 for 48 hours and 1.596 ± 0.168 for 72 hours. For each NP quantity (8 or 16 µg), means with different letters are significantly different from one another ($p<0.05$) as determined by analysis of variance followed by a post-hoc Newman-Keuls test.

See table 1 for NPs acronyms. C, control cells (black line); 8 µg, 16 µg, were the quantity of various NPs added to 100,000 cells.

When the cells were treated with SPIONs coated or not with silica and capped or not with CLA, the reduction of viability is higher in cells treated with Fe_3O_4+CLA2 than in the cells treated with other ones. No significant difference was found between 48 and 72 hours for cells treated with SPIONs+CLA for both quantity of NPs. The NP internalization by cells was evidenced with iron staining (Figure 6). NPs functionalized or not with CLA are present in the cells, whereas no staining is evident in cells untreated with NPs. The analysis by gas chromatography-mass spectrometry of

lipids extracted from 4T1 cells incubated with SPIONs coated or not with silica and capped or not with CLA shows that CLA is incorporated in lipids, and it is higher in cells treated with Fe_3O_4+CLA2 in comparison with cells treated with Fe_3O_4+CLA1 NPs (Table 2). With regards the incorporation of CLA in lipids extracted from 4T1 cells incubated with Fe_3O_4-SiO_2+CLA2, the Table 2 showed a lesser incorporation of CLA for isomer 1 and 2 and a slight increase for the isomer 3.

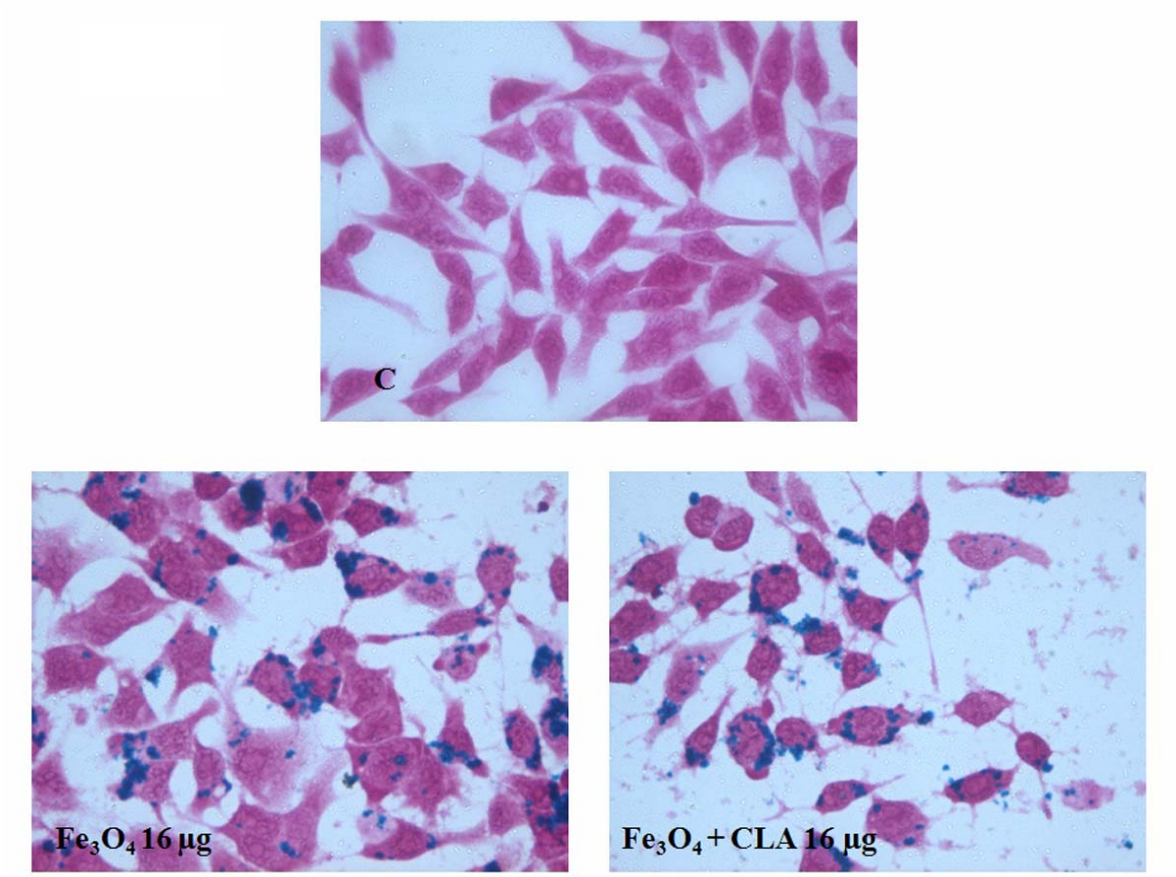

Figure 6. Iron staining. Prussian blue staining was used to evidence the presence of SPIONs with and without silica capped or not with CLA in the mouse breast cancer 4T1 cells. It was reported only the iron staining relative to 16 µg/100,000 cells of various SPIONS after 72 hours of treatment. C, control cells without SPIONs; see table 1 for NPs acronyms.

Table 2: Conjugated linoleic acid (CLA) in lipids extracted from 4T1 cells treated for 72 hours with SPIONS coated or not with silica and capped or not with CLA.. The values are means of two experiments and are expressed as number of times the control cells (C) set equal to 1. See legend in table 1 for NPs acronyms. 16 µg were the quantity of NPs added to 100,000 cells.

Sample	CLA: 3 isomers		
	Isomer n. 1	Isomer n. 2	Isomer n. 3
C	1	1	1
Fe_3O_4 16 µg	0.90	0.72	0.68
Fe_3O_4+CLA1 16 µg	1.97	15.30	1.08
Fe_3O_4+CLA2 16 µg	2.75	19.70	1.26
Fe_3O_4-SiO_2+CLA2 16 µg	1.52	1.64	1.61

The effect of CLA alone on 4T1 cell viability is reported in Table 3. Two concentrations of CLA similar to the quantity used for the preparation of SPIONS were added to the 4T1 cells. A time-dependent reduction of cell viability was observed.

Table 3 Viability of mouse breast cancer 4T1 cells exposed to CLA

Sample	24 h	48 h	72 h
C	100	100	100
CLA 10 µM	91.7	69.1	72.0
CLA 25 µM	86.5	69.2	69.5

The values are means of 2 experiments and are expressed as % of control cells set equal to 100 %. The absorbance values of control are 0.591 ± 0.192 for 24 hours, 1.457 ± 0.151 for 48 hours and 1.596 ± 0.168 for 72 hours.

C, control cells.

To verify whether the different types of SPIONS affected in different way normal and cancer cells, pancreatic islet endothelial MS1 cells were treated. For these experiments, only CLA2 (4.5 µl CLA/ ml of NPs) was used. Table 4 shows that no decrease of viability was induced by all types of SPIONS in comparison with control cells. In particular there were no differences between SPIONS capped or not with CLA.

Table 4 Viability of pancreatic islet endothelial MS1 cells exposed to Fe_3O_4 NPs coated or not with silica and capped or not with CLA. The values are means of 2 experiments and are expressed as % of control cells set equal to 100 %. The absorbance values of control are 0.256 for 24 hours, 0.771 for 48 hours and 0.601 for 72 hours.

See table 1 for NPs acronyms. C, control cells; 8 µg, 16 µg, were the quantity of various NPs added to 100,000 cells.

Sample	24 h		48 h		72 h	
	8 µg	16 µg	8 µg	16 µg	8 µg	16 µg
C	100	100	100	100	100	100
Fe_3O_4	97.09	103.41	111.47	103.24	151.99	140.76
Fe_3O_4+CLA2	94.80	104.86	125.76	103.63	146.53	133.11
Fe_3O_4-SiO_2	101.56	110.86	114.02	107.13	127.03	131.44
Fe_3O_4-SiO_2+CLA2	102.94	114.79	118.96	94.16	136.76	148.91

Figure 7 reports that NPs coated or not with silica and capped or not with CLA are present in the MS1 cells.

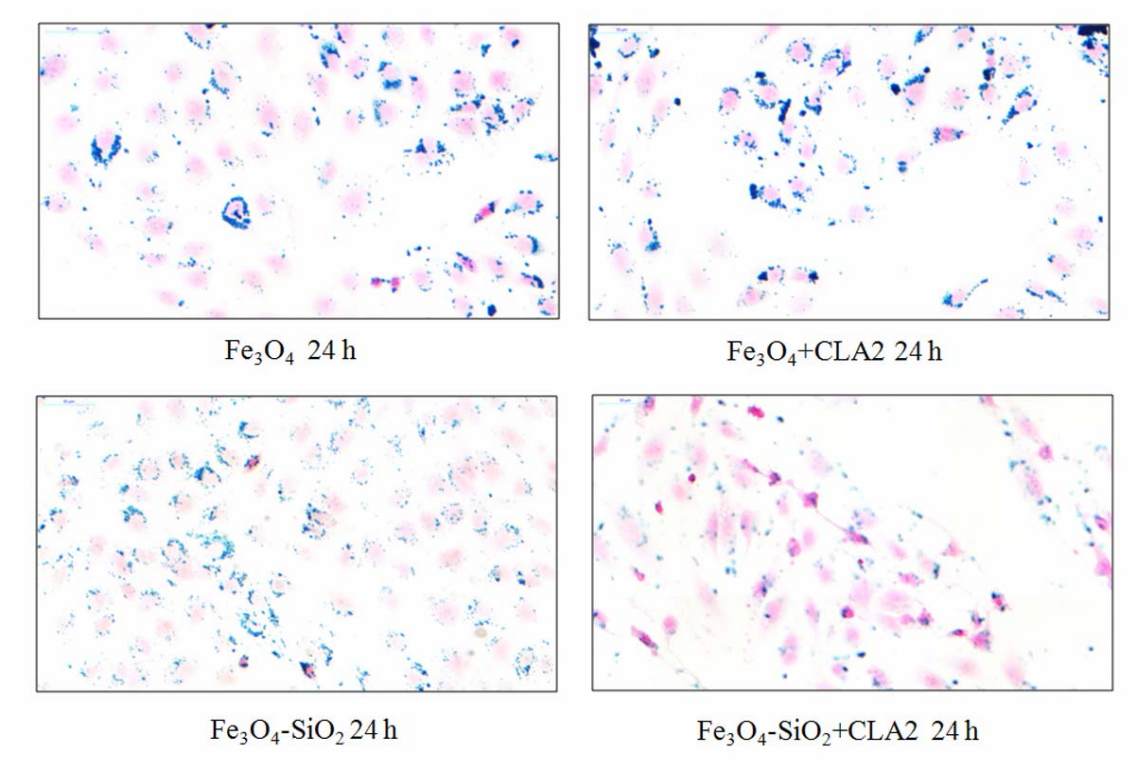

Figure 7. Iron staining for MS1 cells.

Prussian blue staining was used to evidence the presence of SPIONs with and without silica capped or not with CLA in pancreatic islet endothelial MS1 cells.

It was reported only the iron staining relative to 16 µg/100,000 cells of various SPIONS after 24 hours of treatment. See table 1 for NP acronyms.

4. Discussion

In recent years, NPs have been proposed for biomedical utilization [27-31]. This approach implies the synthesis of biocompatible NPs, which are also stable and easily manageable in biological media. For this reason, several coatings have been proposed to improve colloidal stability, prevent oxidation, and improve biocompatibility of NPs [10]. Among them, fatty acids have been also investigated.

Some authors have used OA, which belongs to unsaturated monocarboxylic acids, to functionalize Fe_3O_4 NPs; in particular the study reported by Hemei Chen et al. [32] showed that OA capped

Fe_3O_4 NPs possessed high magnetization and were useful to further adsorb other biomacromolecules. Other studies, instead of using a single adsorption layer of OA, stabilized magnetic NPs by short-chain-length monocarboxylic acids, such as lauric acid and myristic acid [33], but the magnetic NPs were in part aggregated [34]. However, magnetic NPs coated with myristic or lauric acids were cytotoxic for glioblastoma cells, showing low toxicity for normal astrocytes [33]. Starting from the evidence that fatty acids seem biocompatible for healthy cells and toxic for cancer cells, the rationale of their use as capping agent for magnetic NPs should be adjusted, trying to optimize their role as NPs driven therapeutic agents, not only as biocompatible surfactants.

In this study, CLA was chosen as capping agent for magnetic NPs for its antitumor properties [11-13]; its effect on colloidal stability of NPs suspensions and its potential therapeutic effect, when grafted on NPs, were evaluated. The effect of silica coating was also investigated. The superparamagnetic properties of pure Fe_3O_4 NPs were previously assessed [21]. The size and morphology of the NP batch prepared for this research were investigated and a good reproducibility of the results was observed in respect of previous preparations, both for uncoated and silica coated magnetic NPs. The presence of CLA on the magnetic NPs was evidenced by the FT-IR analysis. The results showed the presence of iron oxide and of organic species ascribable to CLA on all samples. It can therefore be assumed that all the functionalization methods were successful. Interestingly it can be evidenced that different signals ascribable to CLA, which could be related to the presence of a single- or bi-layered configuration, were present. All functionalized particles showed the signals related to the CLA main chain (2852 e 2922 cm^{-1} of CH_2 group and 1408 cm^{-1} of CH_3 group [14]). Moreover, in all functionalized NPs also the band ascribed to asymmetric and symmetric stretch vibration of COO^- group (1500-1640 cm^{-1}) appeared [14,22]. This band was not present in the FT-IR spectrum of pure CLA (i.e. not adsorbed on any support) since it can be related to the covalent interaction between COO- groups and Fe atoms in a chelating bidentate interaction

with iron oxide surfaces [22]. The patterns of the Fe_3O_4+CLA1-TS and Fe_3O_4-NW+CLA1-TS revealed signals also present in not adsorbed CLA (1250-1285 cm^{-1} for C-O [22,23] and 1710 cm^{-1} C=O [14]), but absent in the patterns of CLA adsorbed on NPs with a single-step procedure and low CLA content (see for example the patterns of Fe_3O_4+CLA1, Fe_3O_4-NW+CLA1 and [23]), as a demonstration of the presence of free –COOH groups exposed on the NP surface, typical of a bi-layer configuration [14]. The functionalization with highest CLA amount, even in a single step (Fe_3O_4+CLA2 and Fe_3O_4- SiO_2+CLA2), gave FT-IR results similar to Fe_3O_4+CLA1-TS and Fe_3O_4-NW+CLA1-TS NPs both with and without the presence of silica shell. In this case the excess of CLA probably produced a secondary layer, with a configuration similar to the one obtained by the two-step synthesis procedure [14].

The NPs functionalized with CLA in a one step were chosen, among different preparations of SPIONs, because they reduced cell viability more than NPs coated with CLA with two-step procedure (data not shown). Two amounts of CLA (one step) were used: Fe_3O_4+CLA1 (3 µl CLA/ml of NPs) and Fe_3O_4+CLA2 (4.5 µl of CLA/ml of NPs). The results obtained showed that both Fe_3O_4+CLA1 and Fe_3O_4+CLA2 reduced the cell viability of 4T1 cells treated for 24 and 72 hours, respect to control cells not incubated with SPIONs and to 4T1 cells incubated with SPIONs without CLA, but Fe_3O_4+CLA2 was more effective in the reduction than Fe_3O_4+CLA1. For Fe_3O_4+CLA2, the viability values were not significantly different between 48 and 72 hours. A similar trend was observed in 4T1 cells treated with CLA alone.

To be noted that the experiments, carried out to evaluate the effect of various SPIONS on normal cells, showed that SPIONS capped or not with CLA2 and coated or not with silica did not decrease the viability of the normal MS1 cells.

The NP precipitation time with both CLA amounts was also determined. Although all the particles seem aggregated in STEM images of Figure 1 suspensions stable up to 24h were obtained (Figure 4), as discussed in the following. This observation may be explained by the fact that STEM images

of the particles were obtained after drying a drop (5 µl) of the suspension onto a carbon coated copper TEM grid. Upon drying onto a substrate particles obviously aggregates and appear as agglomerates in the images.

As shown in Figure 4 the precipitation time was shorter for Fe_3O_4+CLA1 than for Fe_3O_4+CLA2: at 30 min Fe_3O_4+CLA1 NPs were all precipitated, while Fe_3O_4+CLA2 NPs remained in suspension up to 2 hours. This difference can be explained taking into account that Fe_3O_4+CLA2, even if synthesized with one step procedure, were covered by a secondary layer of CLA (see FT-IR results). It can be supposed that the highest amount of CLA caused a condition similar to that of bilayer-coated NPs (even if the bilayer was probably not continuous). It is reasonable that Fe_3O_4+CLA2 NP surface is more hydrophilic in comparison to that of Fe_3O_4+CLA1 ones (which do not expose free -COOH groups) and, in turn, NPs show a better stability in aqueous medium.

The determination, by gas chromatography-mass spectrophotometry, of CLA isomers in the lipids extracted from cells incubated with SPIONs functionalized or not with CLA, showed that this fatty acid was more incorporated in the cells treated with Fe_3O_4+CLA2 NPs than in the cells treated with Fe_3O_4+CLA1 NPs. The results of this study indicate that the use of the highest amount of CLA (4.5 µl/1 ml of NPs) improves the suspension stability, the CLA incorporation into the cells and the antitumor activity. It worth of mentioning that it is very important to avoid the formation of clusters, because they partially lose the magnetic properties, and, when injected intravascularly, show a shorter circulation time due to rapid clearance by monocytes, this decreasing the reaching of target cells or tissues.

Interestingly the NPs coated with a thin layer of silica and functionalized with CLA showed a further increase of time required to have the precipitation, in fact at 24 hours Fe_3O_4-SiO_2+CLA2 NPs were all dispersed in solution. This effect can be mainly attributed to the citric acid functionalization needed for silica coating, and cannot be ascribed exclusively to CLA amount. Fe_3O_4-SiO_2+CLA2 NPs also cause a reduction of cell viability in comparison with control cells and

CLA-free Fe_3O_4-SiO_2, but the inhibition was lower than that obtained with Fe_3O_4+CLA2. In the same way, the incorporation of CLA in lipid extracted from the cells treated with Fe_3O_4-SiO_2+CLA2 NPs was lower for the isomers 1 and 2 than that obtained with Fe_3O_4+CLA2.

This difference could be ascribed to the role of the silica shell avoiding the direct contact between the magnetite NPs and the biological environment, which in turn reduces their potential toxicity.

Moreover, according to the reported data, we can infer that fatty acids may improve the affinity between NPs and cell membrane and favor particle internalization in tumor cells. This is an important issue for future research, for example for studies with other cancer cell lines as well as for magnetic NP-assisted gene therapy, to improve the use of viral vectors to transfer therapeutic genes to target cells [35-37].

5. Conclusions

In this research colloidal suspensions of Fe_3O_4 NPs, both uncoated or coated by silica shell, of about 5-20 nm in diameter, were successfully prepared and functionalized with different amounts of CLA both in single- and bi-layer configurations. Both the silica shell and CLA layer played a role in determining suspension stability, especially when CLA was grafted on the NP surface in a bi-layer configuration. The results evidenced that the viability of mouse breast cancer 4T1 cells was reduced in presence of Fe_3O_4 NPs functionalized with CLA in comparison with both untreated control cells and cells treated with CLA-free NPs. The presence of the silica coating in CLA capped NPs caused a lesser inhibition of cell viability. Since it is known that the colloidal stability must be assured to avoid uncontrolled NPs clusterization, loosening of magnetic properties and short circulation time, control of this parameter is crucial, even if it is not directly related to the antitumoral effect observed in this work. Based on these results, silica shell free Fe_3O_4 NPs functionalized with high amount of CLA (with bi-layered configuration) can be suggested as therapeutic carriers for their good dispersion and ability to decrease mouse breast cancer 4T1 cell viability.

6. Acknowledgments

This work was supported by grants from AIRC, Italy: IG n. 13166, “Development of engineered magnetic nanoparticles for cancer therapy”, http://www.airc.it to A.F., from Compagnia di San Paolo, Italy, and from the University of Turin, Italy.

7. References

[1] Kandasamy G and Maity D 2015 Recent advances in superparamagnetic iron oxide nanoparticles (SPIONs) for in vitro and in vivo cancer nanotheranostics *Int. J. Pharm*. 496 191-218.

[2] Schroeder A, Winslow MM, Dahlman JE, Pratt GW, Langer R, Jacks T and Anderson DG 2012 Treating metastatic cancer with nanotechnology *Nat. Rev. Cancer*. 12 39-50.

[3] Pietronave S, Locarno D, Rimondini L and M. Prat 2009 Functionalized nanomaterials for diagnosis and therapy of cancer *J. Appl. Biomater. Biomech*. 7 77-89.

[4] Tefft BJ, Uthamaraj S, Harburn JJ, Klabusay M, Dragomir-Daescu D and. Sandhu GS 2015 Cell Labeling and Targeting with Superparamagnetic Iron Oxide Nanoparticles *J. Vis. Exp*. doi: 10.3791/53099.

[5] Brown BD and Naldini L 2009 Exploiting and antagonizing microRNA regulation for therapeutic and experimental applications *Nat. Rev. Genet*. 10 578-585.

[6] Maity D, Chandrasekharan P, Pradhan P, Chuang KH, Xue JM, Feng SS and Ding J 2011 Novel synthesis of superparamagnetic magnetite nanoclusters for biomedical applications *J. Mater. Chem*. 21 14717-14724.

[7] Majeed J, Pradhan L, Ningthoujam RS, Vatsa RK, Bahadur D and Tyagi AK 2014 Enhanced specific absorption rate in silanol functionalized Fe3O4 core-shell nanoparticles: Study of Fe

leaching in Fe3O4 and hyperthermia in L929 and HeLa cells, Colloids Surf. B Biointerfaces. 122 396–403.

[8] Landázuri N, Tong S, Suo J, Joseph G, Weiss D, Sutcliffe DJ, Giddens DP, Bao G and Taylor WR 2013 Magnetic targeting of human mesenchymal stem cells with internalized superparamagnetic iron oxide nanoparticles *Small* 9 4017-4026.

[9] Park J, An K, Hwang Y, Park JG, Noh HJ, Kim JY, Park JH, Hwang NM, Hyeon T 2004 Ultra-large-scale syntheses of monodisperse nanocrystals *Nat. Mater.* 3 891–895.

[10] Wu W, Wu Z, Yu T, Jiang C and Kim WS 2015 Recent progress on magnetic iron oxide nanoparticles: synthesis, surface functional strategies and biomedical applications *Sci. Technol. Adv. Mater.* 16 023501.

[11] Belury MA 2002 Inhibition of carcinogenesis by conjugated linoleic acid: potential mechanisms of action *J. Nutr.* 132 2995-2998.

[12] M. Maggiora et al., 2004 An overview of the effect of linoleic and conjugated-linoleic acids on the growth of several human tumor cell lines *Int. J. Cancer.* 112 909-919.

[13] Muzio G, Oraldi M, Trombetta A and Canuto RA 2007 PARalpha and PP2A are involved in the proapoptotic effect of conjugated linoleic acid on human hepatoma cell line SK-HEP-1 *Int. J. Cancer*. 121 2395-2401.

[14] Yang K, Peng H, Wen Y and Li N 2010 Re-Examination of Characteristic FTIR Spectrum of Secondary Layer in Bilayer Oleic Acid Coated Fe3O4 Nanoparticles *Appl. Surf. Sci*. 256 3093-3097.

[15] Campelj S, Makovec D and Drofenik M 2008 Preparation and properties of water-based magnetic fluids *J. Phys Condens. Matter*. 20 204101 (5pp). doi: 10.1088/0953-8984/20/20/204101.

[16] .Stöber W and Fink A 1968 Controlled Growth of Monodisperse Silica Spheres in the Micron Size Range *Journal of colloidal and interface Science* 26 62-69.

[17] Folch J, Lees M and Sloane Stanley G.H 1957 A simple method for the isolation and purification of total lipides from animal tissues *J.Biol. Chem*. 226 497–509.

[18] Klem S, Klinger M, Demmelmair H and Koletzko B 2012 Efficient and specific analysis of red blood cell glycerophospholid fatty acid composition *PLOSone*. 7 e33874.

[19] Yen TY, Stephen Inbaraj B,. Chien JT and Chen BH 2010 Determination of conjugated linoleic acids and cholesterol oxides and their stability in a model system *Anal. Biochem*. 400 130–138.

[20] Sánchez-Ávila N, Mata-Granadosa, JM, Ruiz-Jiménez J and Luque de Castro MD 2009 Fast, sensitive and highly discriminant gas chromatography–mass spectrometry method for profiling analysis of fatty acids in serum *J. Chromatogr. A.* 1216 6864–6872.

[21] E. Verné et al., 2014 Iron-oxide nanoparticles used for target cancer gene therapy and hyperthermia, Proceedings of the 29th annual meeting of the European Society for hyperthermic oncology, Minerva Med. 56 16.

[22] Zhang L, He R and Gu HC 2006 Oleic acid coating on the monodisperse magnetite nanoparticles *App.Surf. Sci.* 253 2611-2617.

[23] Korolev VV, Ramazanova AG and Blinov AV 2002 Adsorption of surfactants on superfine magnetite *Russ. Chem. Bull. (Int. Ed.).* 51 2044-2049.

[24] Kadamne JV, Castrodale CL and Proctor A 2011 Measurement of Conjugated Linoleic Acid (CLA) in CLA-Rich Potato Chips by ATR-FTIR Spectroscopy *J. Agric. Food Chem.* 59 2190–2196.

[25] Mojic B, Giannakopoulos KP, Cvejic Z and Srdic VV 2012 Silica coated ferrite nanoparticles: Influence of citrate functionalization procedure on final particle morphology *Ceram. Int.* 38 6635-6641.

[26] Fatemeh A. Ali H.and Sirous N 2013 Surface modification of Fe3O4@SiO2 microsphere by silane coupling agent *Int. Nano Lett.* 3 23.

[27] Mornet S, Vasseur S, Grasset F, Veverka P, Goglio G, Demourgues A, Portier J, Pollert E and Duguet E 2006 Magnetic nanoparticles design for medical applications *Prog. Solid State Chem*. 34 237–247.

[28] Wuang SC,. Neoh KG, Kang ET, Pack DW and Leckband DE 2006 Heparinized Magnetic Nanoparticles: In-Vitro Assessment for Biomedical Applications *Adv. Funct. Mater*. 16 1723–1730.

[29] Duguet E, Vasseur S, Mornet S and Devoisselle JM 2006 Magnetic nanoparticles and their applications in medicine *Nanomedicine* 1 157–168.

[30] Fortin JP, Wilhelm C, Servais J, Ménager C, Bacri JC and Gazeau F. 2007 Size-Sorted Anionic Iron Oxide Nanomagnets as Colloidal Mediators for Magnetic Hyperthermia *J. Am. Chem. Soc.* 129 2628–2635.

[31] Brusentsov NA, Nikitin LV, Brusentsova TN, Kuznetsov AA, Bayburtskiy FS and Shumakov LI, Jurchenko NY 2002 Magnetic field hyperthermia of the mouse experimental tumor, *J. Magn. Magn. Mater*. 252 378–380.

[32] Chen H, Liu S, Li Y, Deng C, Zhang X and Yang P 2011 Development of oleic acid-functionalized magnetite nanoparticles as hydrophobic probes for concentrating peptides with MALDI-TOF-MS analysis *Proteomics* 11 890–897.

[33] Avdeev MV, Lamszus K, Vekas L, Garamus VM, Feoktystov AV, Marinica O, Turcu R and Willumeit R 2010 Structure and in vitro biological testing of water-based ferrofluids stabilized by monocarboxylic acids *Langmuir* 26 8503-8509.

[34] Bica D, Vekas L, Avdeev MV, Marinic O, Socoliuc V, Balasoiu M and Garamus VM 2007 Sterically stabilized water based magnetic fluids: Synthesis, structure and properties, *J. Magn. Magn. Mater.* 311 17–21.

[35] Wiznerowicz M and Harnessing TD 2005 HIV for therapy, basic research and biotechnology *Trends Biotechnol.* 23 42-47.

[36] Follenzi A, Ailles LE, Bakovic S, Geuna M and Naldini L 2000 Gene transfer by lentiviral vectors is limited by nuclear translocation and rescued by HIV-1 pol sequences *Nat. Genet.* 25 217-222.

[37] Follenzi A and Naldini L 2002 HIV-based vectors. Preparation and use *Methods Mol. Med*. 69 259-274.

Figure Captions

Figure 1. STEM images of SPIONs.

Fe_3O_4+CLA1, washed CLA-capped Fe_3O_4 NPs; Fe_3O_4-NW+CLA1, not washed CLA-capped Fe_3O_4 NPs; Fe_3O_4+CLA1-TS, washed two step CLA-capped Fe_3O_4 NPs; Fe_3O_4-NW+CLA1-TS NPs, not washed two step CLA-capped Fe_3O_4 NPs; Fe_3O_4+CLA2; Fe_3O_4-SiO_2+CLA2, silica shell-coated, washed CLA-capped Fe_3O_4 NPs.

CLA1, 3.0 µl of CLA/ml of NPs; CLA2, 4.5 µl of CLA/ml of NPs.

Figure 2. FT-IR spectra.

(a) FT-IR spectra of pure CLA; (b) whole spectrum of Fe_3O_4-NW+CLA1 (curve I), Fe_3O_4-NW+CLA1-TS (curve II), Fe_3O_4+CLA1 (curve III), Fe_3O_4+CLA1-TS (curve IV) NPs; (c) selected windows between 1000 and 4000 cm^{-1}.

See table 1 for NPs acronyms.

Figure 3. FT-IR spectra.

FT-IR spectra of Fe_3O_4+CLA2 (curve I) and Fe_3O_4-SiO_2+CLA2 (curve II) NPs.

See table 1 for NPs acronyms.

Figure 4. Precipitation of SPIONs

Time of precipitation of NPs with or without silica, capped or not with CLA

See table 1 for NPs acronyms.

Figure 5 Viability of mouse breast cancer 4T1 cells exposed to Fe_3O_4 NPs coated or not with silica and capped or not with CLA.

The values are means ± S.D. of 4 experiments and are expressed as % of control cells set equal to 100 %. The absorbance values of control are 0.591 ± 0.192 for 24 hours, 1.457 ± 0.151 for 48 hours and 1.596 ± 0.168 for 72 hours.

For each NP quantity (8 or 16 µg), means with different letters are significantly different from one another ($p<0.05$) as determined by analysis of variance followed by a post-hoc Newman-Keuls test.

See table 1 for NPs acronyms.

C, control cells (black line); 8 µg, 16 µg, were the quantity of various NPs added to 100,000 cells.

Figure 6. Iron staining.

Prussian blue staining was used to evidence the presence of SPIONs with and without silica capped or not with CLA in the mouse breast cancer 4T1 cells.

It was reported only the iron staining relative to 16 µg/100,000 cells of various SPIONS after 72 hours of treatment.

C, control cells without SPIONs; see table 1 for NP acronyms.

Figure 7. Iron staining for MS1 cells.

Prussian blue staining was used to evidence the presence of SPIONs with and without silica capped or not with CLA in pancreatic islet endothelial MS1 cells.

It was reported only the iron staining relative to 16 µg/100,000 cells of various SPIONS after 24 hours of treatment.

See table 1 for NP acronyms.